ARTICLE

BIOTECHNOLOGY and BIOENGINEERING

Physiological Responses of CHO Cells to Repetitive Hydrodynamic Stress

Ruben Godoy-Silva,[1,2] Jeffrey J. Chalmers,[2] Susan A. Casnocha,[1] Laura A. Bass,[3] Ningning Ma[1]

[1]Bioprocess R&D, Global Biologics, Pfizer, Inc., 700 Chesterfield Parkway West, Chesterfield, Missouri 63017; telephone: 636-247-8209; fax: 636-247-6098; e-mail: ningning.ma@pfizer.com

[2]Department of Chemical and Biomolecular Engineering, The Ohio State University, Columbus, Ohio

[3]Analytical R&D, Global Biologics, Pfizer, Inc., Chesterfield, Missouri

Received 26 January 2008; revision received 3 March 2009; accepted 23 March 2009

Published online 3 April 2009 in Wiley InterScience (www.interscience.wiley.com). DOI 10.1002/bit.22339

ABSTRACT: A majority of the previous investigations on the hydrodynamic sensitivity of mammalian cells have focused on lethal effects as determined by cell death or lysis. In this study, we investigated the effect of hydrodynamic stress on CHO cells in a fed-batch process using a previously reported system which subjects cells to repetitive, high levels of hydrodynamic stress, quantified by energy dissipation rate (EDR). The results indicated that cell growth and monoclonal antibody production of the test cells were very resistant to the hydrodynamic stress. Compared to the control, no significant variation was observed at the highest EDR tested, 6.4×10^6 W/m^3. Most product quality attributes were not affected by intense hydrodynamic stress either. The only significant impact was on glycosylation. A shift of glycosylation pattern was observed at EDR levels at or higher than 6.0×10^4 W/m^3, which is two orders of magnitude lower than the EDR where physical cell damage, as measured by lactate dehydrogenase release, was observed. While not as extensively investigated, a second monoclonal antibody produced in a different CHO clone exhibited the same glycosylation change at an intensive EDR, 2.9×10^5 W/m^3. Conversely, a low EDR of 0.9×10^2 W/m^3 had no effect on the glycosylation pattern. As 6.0×10^4 W/m^3, the lowest EDR that triggers the glycosylation shift, is about one order of magnitude higher than the estimated, maximum EDR in typically operated, large-scale stirred tank bioreactors, further studies in a lower EDR range of 1×10^3–6.0×10^4 W/m^3 are needed to assess the glycosylation shift effect under typical large-scale bioreactor operation conditions. Follow-up studies in stirred tanks are also needed to confirm the glycosylation shift effect and to validate the repetitive hydrodynamic stress model.

Biotechnol. Bioeng. 2009;103: 1103–1117.

KEYWORDS: Mammalian cell culture; CHO; hydrodynamic stress; physiological response; glycosylation; shear sensitivity

Introduction

Since established nearly 30 years ago, mammalian cell culture for recombinant protein production has rapidly evolved into an important platform to produce modern biopharmaceuticals. For monoclonal antibodies alone, there are over 160 molecules in various stages of clinical trials and the projected revenue in 2012 could exceed $40 billion (Datamonitor, 2007). Over the same time span, mammalian cell culture technology has also evolved rapidly (Wurm, 2004). For example, in fed-batch processes, peak cell densities have increased by over an order of magnitude from millions of cells/mL to ten(s) of millions/mL and product titer has increased over three orders of magnitude from mg/L to g/L. However, a fundamental question, regarding degree of sensitivity of industrial cell lines to hydrodynamic stress, is still waiting to be fully answered. Even though many processes have been successfully scaled up to bioreactors as large as 25,000 L, agitation in many large-scale bioreactors might not be operated at an optimal condition for mixing in an effort to avoid "shear damage". With peak cell density continuing to increase in bioprocesses, the requirement for more intensive agitation may be important to ensure adequate mixing and mass transfer.

The intensity of agitation a particular cell line can withstand depends on two factors. One is the maximum local hydrodynamic force produced by a specific agitation

Ruben Godoy-Silva's present address is National University of Columbia, Bogota, Columbia.

Correspondence to: N. Ma

condition and the other is the hydrodynamic sensitivity of the cells. In a stirred tank bioreactor, mechanical energy is transferred from impellers to the liquid and then dissipated through a series of eddy cascades, which eventually converts all mechanical energy into thermal energy, heat. Energy dissipation is the driving force for mixing and also the cause of the hydrodynamic stress on the cells. Local energy dissipation in stirred tanks shows great heterogeneity. Impeller regions, albeit accounting for only about 10% tank volume, could account for up to 70% of total energy dissipation. Therefore, the local maximum energy dissipation rate in the impeller region could be two orders of magnitude higher than the volumetric average energy dissipation rate (Wernersson and Tragardh, 1999; Zhou and Kresta, 1996a,b).

Liquid renewal rate in the impeller region is high; therefore, the exposure of cells to intense energy dissipation is short. Transient flow through microfluidic channels is a useful model for producing a brief, but intensive, energy dissipation environment for studying cell line shear sensitivity. In a pioneering work, Augenstein et al. (1971) tested two mammalian tissue cell lines, HeLa S3 and mouse L929, using a set of capillary tubes with different bore sizes. Cell damage was observed at average wall shear stresses between 10 and 200 N/m^2, which are approximately 1×10^5 and 4×10^7 W/m^3. McQueen et al. (1987) and McQueen and Bailey (1989) tested the sensitivity of a mouse myeloma cell line in a sudden contractual and a gradual contractional microfluidic tube. They observed the threshold wall shear for measurable cell lysis was 1,800 and 1,500 dyn/cm^2 respectively, which are approximately 3.2×10^7 and 2.2×10^7 W/m^3. More recently, Chalmers and co-workers designed a set of transient contractional microfluidic channels, where hydrodynamic stress in the contractional region was characterized (Ma et al., 2002; Mollet et al., 2007). These flow devices, dubbed ''torture chambers,'' were used to quantify the hydrodynamic sensitivity of cell lines relevant to biopharmaceutical production, including CHO-K1 wild type and bcl-2 transformed, hybridoma, and PER.C6 (Ma, 2002; Ma et al., 2002; Mollet et al., 2007). In general, an energy dissipation rate above 2.0×10^6 W/m^3 was observed to elicit detectable cell lysis. This is much higher than the maximum level that can be generated by agitation in bioreactors, suggesting that agitation in large-scale bioreactor is not responsible for physical death of these cells. However, cell sensitivity to hydrodynamic stress measured in these studies could be underestimated for two reasons. First, cells were forced through the torture chamber for only a single passage, while in bioreactors the hydrodynamic force that cells are subjected to is maintained throughout the entire production process. Second, these studies defined cell damage as acute cell lysis, measured by release of lactate dehydrogenase (LDH). However, the question of whether sublethal effects, such as productivity or product quality change, might be triggered by lower level EDR has not been addressed. Godoy-Silva et al. (2009) developed a bioreactor recirculation system which subjects cells to repetitive, high level hydrodynamic exposure. Using this model, Godoy-Silva et al. (2009) tested the effect of repetitive hydrodynamic stress on the growth and recombinant protein production of a CHO cell line. They observed that cell growth was negatively impacted at energy dissipation rate (EDR) levels 1–2 orders of magnitude lower than that required to lyze the cells under single transient exposure. At 2.9×10^5 W/m^3, apparent cell growth stopped and at 2.3×10^6 W/m^3, cell death was observed. In another study, the minimal flow rate through a capillary tube that was required to lyze CHO cells was found lower under multiple-passage condition than that under single-passage condition (Vickroy et al., 2007). It was also found that cells in low viability cultures were easier to lyze. In addition to microfluidic channels, there were other tools, especially viscometers, that had been used for hydrodynamic sensitivity studies. These studies have been reviewed previously (Chalmers, 2000; Chisti, 1999, 2000; Joshi et al., 1996; Ma et al., 2006; Varley and Birch, 1999).

Studies that investigated sublethal effects of hydrodynamic stress on mammalian cells are limited. Even more unsatisfactory, most of these studies are for medical or cell physiology purposes, so that the cell lines, test protocol, and the sublethal effects monitored were not directly relevant to bioprocess applications. Nevertheless, these studies did reveal that sublethal effects can be triggered by lower level hydrodynamic forces than that lethal effects need. As summarized in Ma et al. (2002), shear stress at 1.0–10 N/m^2, which correlates to approximately 1×10^3–1×10^5 W/m^3, could elicit sublethal physiological responses. This is significantly lower than the level required to lyze similar cell lines. Of bioprocess relevant cell lines, Ranjan et al. (1996) found an induction of transcriptional activator c-fos when CHO cells were subjected to 2.5 N/m^2 (6.2×10^3 W/m^3) shear force for 1 h. Ludwig et al. (1992) observed morphologically that the time for adherent BHK-21 cells to spread after division increased when the cells were exposed to 4.5 N/m^2 (2.0×10^4 W/m^3). Al-Rubeai et al. (1995) detected apoptosis of hybridoma cells at volumetric average energy dissipation of 1.87×10^3 W/m^3. Motobu et al. (1998) observed that after 24 h exposure to 0.02 and 0.082 N/m^2 (0.4 and 6.5 W/m^3) shear force, nonconfluent CHO cells were arrested at G_0/G_1 phase and mRNA level for the recombinant product was increased, but confluent CHO cells did not respond to the same levels of shear force. Keane et al. (2003) subjected attached CHO cells to shear force for 32 h and monitored recombinant human growth hormone production and glucose metabolism. They observed that when shear force was increased from 0.005 N/m^2 (0.02 W/m^3) to 0.80 N/m^2 (6.4×10^2 W/m^3), recombinant protein production rate was reduced by 51%, glucose uptake rate was increased by 42%, and lactate production was decreased by 50%.

In this study, we used the bioreactor recirculation system to test the hydrodynamic sensitivity of an industrial CHO cell line in a fed-batch process. While lethal effects were

monitored by LDH release, apoptosis, and culture viability decrease, the focus of this study was on the physiological effects associated with process performance and product quality. The process performance factors include net cell growth rate, monoclonal antibody (mAb) production rate, and metabolic state (exemplified by glucose consumption rate and lactate production rate). The product quality factors include aggregation and fragmentation, charge profile, N-linked glycosylation profile, and methionine oxidation. The ultimate goal of this study was to evaluate lethal and sub-lethal effects of varied energy dissipation rates on CHO cells in a model system designed to provide cycled hydrodynamic stress that may represent a simulation of the circulation in a large-scale stirred bioreactor.

Materials and Methods

Cells and Cell Culture Process

A clonal CHO cell line expressing a test mAb was used in this study. The inoculum train was maintained by subculturing cells routinely in a chemically defined medium in vented shake flasks (Corning, Acton, MA) in a CO_2 incubator. Two 2 L bioreactors with 1 L working volume (Applikon, Inc., Foster city, CA) were used as the production bioreactors. The process is a chemically defined fed-batch process. Mixing in the bioreactors was provided by dual pitched blade impellers, 2 inch in diameter, at 130 rpm. Temperature was maintained at 36.5°C using a heating blanket. pH is controlled at 7.0 using carbon dioxide sparging through a ring sparger and 0.5 N sodium hydroxide addition. Dissolved oxygen (DO) was controlled at 30% air saturation using oxygen sparging. Cell density, viability, DO, pH, osmolality, and key nutrients and metabolites were monitored daily. Cell samples and spent medium samples were taken daily to perform various in-process assays described in Analytical Assays Section. Final day recombinant mAb's were purified using a Protein-A spin column based Antibody purification kit (Millipore, Billerica, MA) and the purified products were analyzed for product quality as listed in Analytical Assays Section.

Single and Repetitive Exposure Experiment

In this study, three different sizes of microfluidic devices or "torture chambers (TC)" were used (Table I). The smallest one, with a "throat" dimension of 225 μm, has been characterized previously (Mollet et al., 2007). The other two TCs have "throat dimension" of 1.5 ad 2.0 mm respectively, otherwise all of other dimensions are the same as the 225 μm TC. As with the 225 μm TC, flow and local EDR in the two wider microfludic channels at test flow rate were simulated using FLUENT (Lebanon, NH), a computational fluid dynamics program.

As presented previously (Hu et al. 2007; Mollet et al. 2007), using a single EDR value to characterize the stress on the cells passing through the TC at a given flow rate is complex. Mollet et al. (2007) took the approach of using the median value of the maximum EDR that each of 4,000 simulated particles would experience as they flow through the TC. Alternatively, Hu et al. (2007) calculated the weighted average EDR based on the flow rate through five virtual cross sections of the TC. Each of these cross sections was divided into 1,600 subsections to which an EDR value was associated. The percentage of the total volume flow rate that flows through each of these 1,600 subsections was then used to weigh the value of EDR for each subsection. By summing the weighted EDR value of the 1,600 subsections, an average EDR of cells passing through the cross section was determined. Interestingly, both approaches produced very similar values. It should also be noted, however, that for any given average or median value, the range of EDR that any cell can experience is approximately 1 order of magnitude for the 225 μm TC, but several orders of magnitude for the 1.5 and 2 mm TC (with the mean or median value contained within that range). For example, for a flow rate of 30 mL/min in the 225 μm TC, the median, maximum EDR is 2.3×10^6 W/m^3; however the lowest, maximum EDR was 1×10^6 and the highest is 1×10^7 W/m^3. The median EDR for a range of flow rates in the smallest TC, and for 30 mL/min in the two other TC is presented in Table I.

In the single exposure studies, cells were pumped through a torture chamber for only one passage. The resulting LDH release after the exposure was subsequently quantified to represent cell damage. More specifically, cells drawn out of a 2 L bioreactor were immediately spun down in a refrigerated

Table I. Median and range of energy dissipation rates that cells are exposed to in the Torture Chambers at different volumetric flow rates, for the 225 μm, 1.5 mm, and 2.0 mm throat dimensions.

Torture chamber throat size	225 μm						1.5 mm	2.0 mm
Flow rate (mL/min)	3	10	30	50	70	90	30	30
Median of maximum EDR (W/m^3)	6.0×10^4	2.9×10^5	2.3×10^6	6.4×10^6	2.6×10^7	1.1×10^8	90	12
EDR range (W/m^3)	—	3×10^4 to 1×10^6	1×10^6 to 1×10^7	2×10^6 to 2×10^7	5×10^6 to 8×10^7	1×10^7 to 4×10^8	Up to 1.8×10^4	Up to 2.4×10^3
Recirculation frequency (min^{-1})	200	100	33	20	14	11	33	33

centrifuge (Beckman Coulter, Fullerton, CA) at 200*g* for 5 min. The pellet was then resuspended gently into fresh medium at room temperature (~20°C) to a concentration of 5×10^5 cells/mL. A small portion of the solution was retained as a control for cell damage quantification. The remaining solution was divided into 5 portions which were pumped through a torture chamber at 5 different flow rates using a syringe pump (Harvard Apparatus, Holliston, MA). After a steady flow was developed, the effluent was sampled and the percentage of LDH release quantified. The quantification formula was detailed previously (Ma et al., 2002; Mollet et al., 2007).

In repetitive exposure studies, cells were cultured in a 2 L bench-scale bioreactor and constantly recirculated through a torture chamber via an external loop system. The complete system is illustrated in Figure 1 and detailed descriptions can be found in Godoy-Silva et al. (2009). In brief, a recirculation system is attached to a bench-scale bioreactor where a dual-syringe syringe pump with synchronized dual-solenoid valves provided a unidirectional flow of cell broth from the bench-scale bioreactor through the torture chamber and then back to the bioreactor. A syringe pump, rather than a peristaltic pump, was chosen in this system as the former one provides much more steady flow. A constraint of the recirculation system is that the exposure frequency of cells in the TC was dictated by the desired EDR.

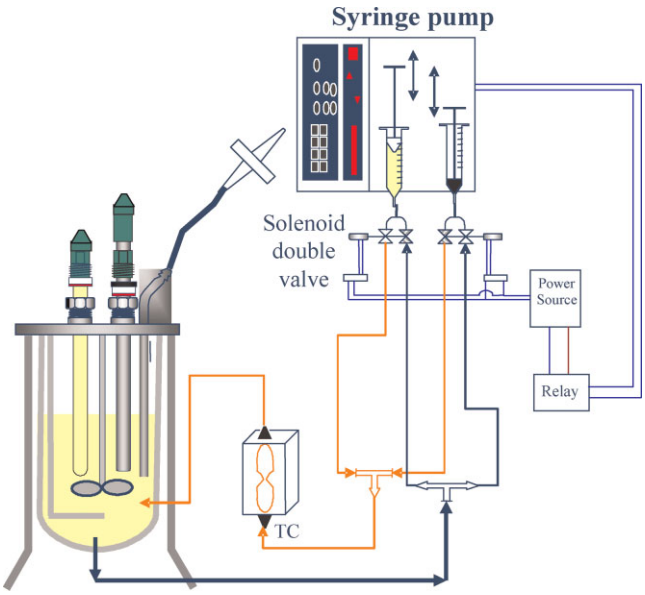

Figure 1. Equipment setup for scale-down repetitive exposure model. An external recirculation loop was attached to a benchtop 2 L bioreactor, where cell culture broth was constantly withdrawn from the bioreactor, pushed through a microfluidic device, Torture Chamber (TC), and returned back into the bioreactor. The unidirectional flow was achieved through using a duel-syringe syringe pump and a solenoid double valve system that was synchronized with the syringe pump. Both syringes were operated bidirectionally but they were always in opposite direction. The solenoid valve system constantly connect the pulling syringe to the inlet cell broth and the pushing one to the Torture Chamber. [Color figure can be seen in the online version of this article, available at www.interscience.wiley.com.]

The average frequency of cells passing through the torture chamber is listed in Table I.

As a control, a companion control bioreactor-recirculating system, minus the TC, but otherwise identical to the bioreactor-recircualting-TC system was run in parallel. In most studies, the control bioreactor and the test bioreactor were operated side by side, using the same inoculum source, lot of medium and nutrient feed. In addition, both systems were operated by the same scientist.

In the first 4 days of the fed-batch process, recirculation was off for both the test and control bioreactors. This period of time was used to confirm that cells were behaving similarly in both bioreactors so that later differentiation between the test and control bioreactors could be attributed to hydrodynamic stress with higher confidence. Recirculation in both bioreactors started on the fourth day and continued to the end of the process.

Analytical Assays

The effects of energy dissipation on the fed-batch process were assessed from two perspectives, lethal and sub-lethal. Lethal effects include necrosis and apoptosis. Sublethal effects include variation in net growth rate, metabolism, antibody production rate, and product qualities. Cell density, viability, and average cell diameter were monitored daily using a Cedex automatic cell counter (Innovatis, Bielefeld, Germany). Offline pH, dissolved oxygen, carbon dioxide, glucose, and lactate were monitored daily using a BioProfile Chemical Analyzer (Nova Biomedical, Waltham, MA). Antibody titer from days 6 to 14 was analyzed using an Agilent HPLC (Hewlett Packard, Waldbronn, Germany) with a POROS protein-A affinity column (Applied Biosystems, Foster City, CA).

LDH Release

A non-radioactive cytotoxicity assay kit (Promega Corp., Madison, WI) and a spectrophotometer (Spectramax 250, Molecular Devices Corp., Sunnyvale, CA) were used to quantify LDH release. During each set of bioreactor runs, daily supernatant samples were collected by gently spinning cells down first at 250*g* for 10 min and then filtering the top portion through a 0.2 μm polyethersulfone filter (Pall, Ease Hills, NY). The samples were stored at −80°C. After the experiment, all samples were thawed and analyzed simultaneously. First, all samples were thawed at 37°C. For samples taken in the first 6 days of the fed-batch process, 50 μL supernatant was directly transferred into a 96-well plate. For samples taken after day 6 of the fed-batch process, a smaller volume was transferred to the 96-well plate where it was diluted with fresh medium to reach 50 μL final volume. The dilution factor was determined empirically from previous experiments and was used to convert the absorbance of diluted samples back to undiluted values. A calibration curve was made before each set of measurement.

Absorbance of all samples was confirmed within the linear range of the titration curve. Fresh samples and −80°C stored samples were compared, which demonstrated that −80°C storage did not alter LDH level in the samples.

Apoptosis

Apoptosis was determined using a Guava EasyCyte Plus flow cytometer and the Guava Nexin assay kit (Guava Technologies, Inc., Hayward, CA). The nexin assay uses two dyes, 7-AAD and phycoerythrin (PE) which is covalently linked to Annexin V. 7-AAD is an indicator of membrane integrity and Annexin V-PE complex has a high affinity to phosphatidylserine (PS), a marker of early apoptosis when detected in external cell membrane. Healthy, non-apoptotic cells are negative for both Annexin V-PE and 7-AAD dyes. Early apoptotic cells are positive for Annexin V-PE, but negative for 7-AAD. Late apoptotic/necrotic cells are positive for both dyes.

The Apoptosis assay was conducted daily using fresh cells from the control and test bioreactors side by side. Manufacturer's instructions were followed. Briefly, 2×10^6 cells were centrifuged at 400*g* and 4°C for 10 min and the cell pellet was resuspended in 1 mL ice-cold Nexin 1× buffer. Sixty four microliters cell suspension was then mixed with 8 μL Annexin V-PE and 8 μL 7-AAD solution in a micro centrifuge tube. After a 20-min incubation on ice, 720 mL cold Nexin 1× buffer was added to each tube and mixed gently. The samples were then read in the Guava EasyCyte Plus System using the Guava Express Plus software. A positive control and a negative control were included in each set of assays. The positive control was prepared by heating healthy cells (from the inoculum train) at 42°C for 50 min and then incubating the cells at normal temperature, 36.5°C, for 6–8 h. The negative control used healthy cells from the inoculum train without staining. Single and dual staining of the positive control was used to adjust the compensation and the gain of the photomultiplier. Negative control was used to set gates for both Annexin V-PE and 7-AAD absorbance.

Molecular Weight Variants

Sodium dodecyl sulfate–polyacrylamide gel electrophoresis (SDS–PAGE), both reduced and nonreduced, was used to detect mass related variants of the product. SDS–PAGE can typically resolve the parent protein (monomer) from covalent aggregates, free heavy chain, free light chain, and fragments. Protein-A purified mAbs were first treated with SDS (Bio-Rad Laboratories, Hercules, CA). For non-reducing SDS–PAGE samples, Iodoacetamide (IAM) (Sigma–Aldrich Corp., St. Louis, MO) was added to minimize disulfide shuffling. For reducing SDS–PAGE, NuPAGE reducing agent (Invitrogen Corp., Carlsbad, CA) was added to break disulfide bonds. The treated samples were then analyzed on a Mini-Gel Apparatus (Invitrogen Corp.) using NuPAGE 4–12% Bis-Tris Gels (Invitrogen Corp.). Proteins were stained with a silver stain kit (Owl Separation Systems, NH) where the images were captured by a densitometer (Bio-Rad Laboratories, Hercules, CA).

Methionine Oxidation

A proteolytic mapping HPLC method was used to quantify oxidized methionyl residues at a specific location in the Fc region. The purified mAb was digested enzymatically using Lysyl endoproteinase-C (Wako Chemicals, Richmond, VA). The resulting peptide fragments were separated by reversed-phase HPLC using a C4 column (Grace Vydac, Deerfield, IL). The peptide fragments containing the specific methionine, or its respective oxidized form, were detected using ultraviolet absorbance. The level of methionine oxidation was quantified as the percentage of the peak area of oxidized fragment to the total peak area of oxidized and parent fragment.

Glycosylation

N-glycosylation profiles were determined using a size exclusion chromatography (SE-HPLC) coupled with mass spectrometry. First, the purified product was reduced using DL-Dithiothreitol (Sigma–Aldrich Corp.). Heavy chains with N-linked glycans were segregated from light chains using SE-HPLC. A super SW3000 (Tosoh Biosciences, Montgomeryville, PA) size exclusion column was used with 60% ACN/0.1% TFA as the mobile phase. The heavy chains were subsequently analyzed using an ESI-Q-TOF mass spectrometer (Waters, Milford, MA). The resulting spectrum was deconvoluted and peaks were identified based on the theoretical molecular weights of the heavy chain and various glycoforms. Percent of a specific glycan is quantified as the ratio of the peak height of this glycan to the combination of all peaks.

Charge Heterogeneity

An imaged capillary isoelectric focusing (iCE) assay was used to monitor protein charge heterogeneity. Purified mAb's are focused within a capillary column in an iCE280 analyzer (Convergent Bioscience, Toronto, Canada) under DC current voltage. Electrophoretic peaks formed by mAb's with different pI's are detected using a whole column ultraviolet light absorbance at 280 nm. The intensity of UV absorbance along the column is then converted to a spectrum. Peak areas are used to determine the relative abundance of parent isoforms, total acidic isoforms, and total basic isoforms.

Results

Single Exposure Test of CHO Cells at Different Growth Phases

Prior to the chronic exposure study, the sensitivity of the specific CHO clone used for this study to a single exposure

to five different levels of EDR, ranging from 2.9×10^5 to 1.1×10^8 W/m^3, was conducted. The purpose of this single exposure study was three fold: (1) to compare the sensitivity of this CHO clone to other previously tested cell lines, (2) to guide the decision of the EDR range for the chronic exposure studies, and (3) to compare the sensitivity of CHO cells in different growth phases in a typical fed-batch process.

Cells from three growth phases in the 14-day fed-batch process in a 2 L bioreactor were tested. As indicated by the arrows in Figure 2a, cell samples were taken on days 4, 9, and 13 to represent cells in the exponential, stationary, and death phases, respectively. Each cell sample was subjected to five different levels of EDR between 2.9×10^5 and 1.1×10^8 W/m^3 using the 255 μm TC. Damage breakthrough curves based on LDH release, as shown in Figure 2b, were similar although there was slightly more damage for cells in the death phase across the entire EDR range studied. For each cell sample, the damage level was similar at 2.9×10^5 W/m^3 and 2.3×10^6 W/m^3 exposure, which was used to define each sample's damage baseline. Starting from 6.4×10^6 W/m^3, there was a gradual increase in cell damage with increasing EDR for all samples, indicating that the breakthrough point for all three samples was similarly at 2.3×10^6 W/m^3. It should be noted that although cells in the death phase had the same breakthrough EDR point, their damage level was always slightly higher than that of the other two populations. This is most likely due to the existence of dead cells in the sample. We had observed that dead cells gradually leak LDH over time. The leakage might have increased when the dead cells were subjected to hydrodynamic forces.

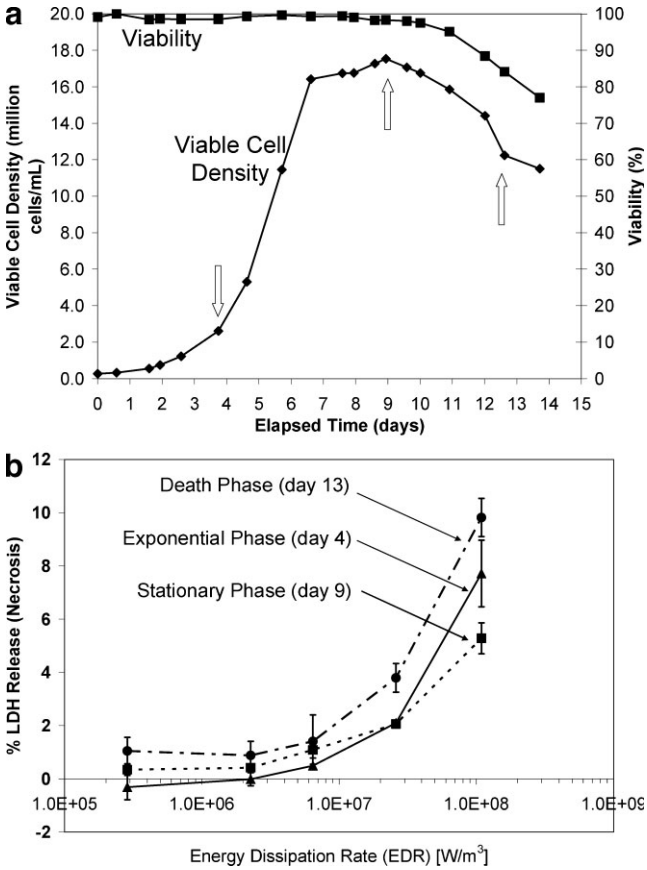

Figure 2. **a**: Viable cell density and viability in a 14-day fed-batch process. The three time points where cells were withdrawn for hydrodynamic sensitivity test are indicated by the arrows. **b**: Hydrodynamic sensitivity of cells taken at three different growth stages. Single exposure model was used where cells were pumped through a Torture Chamber at five different flow rates for a single passage.

Repetitive Exposure of Cells in the Scaled-Down Fed-Batch Process

The single exposure test demonstrated that, similar to previously studies, the industrially relevant CHO clone used in this study was very resistant to hydrodynamic stress with respect to physical cell damage. The threshold EDR for LDH release, 6.4×10^6 W/m^3, is several orders of magnitude higher than the EDR generated by agitation in bioreactors. In the repetitive exposure study, we used the same TC, but at a lower EDR range of 6.0×10^4, 2.9×10^5, 2.3×10^6, and 6.4×10^6 W/m^3.

Cell Growth, Viability, and Productivity

Viable cell density, viability, and normalized product titer of each pair of the control and test bioreactors under four different levels of EDR stress are presented in Figure 3a–d. Product titer was normalized to the highest harvest titer achieved in the total of 8 bioreactor runs. The starting working volume in the 6.0×10^4 W/m^3 experiment was 0.6 L while that in the other three sets of experiments was 1.1 L. The lower working volume at 6.0×10^4 W/m^3 was required since the recirculation rate was significantly lower; thus, lowering the working volume increased cell exposure frequency. Due to the lower working volume, samples were not taken on days 7 and 8 (Fig. 3a) as the sampling port became too close to the liquid surface and foam entered the line during sampling on these 2 days. In all four sets of experiments, cell growth, viability, and product titer were comparable between the test bioreactors and their corresponding control bioreactors.

In general, repetitive exposure to energy dissipation rate up to 6.4×10^6 W/m^3 did not affect cell growth, death, and productivity. At 6.4×10^6 W/m^3, peak cell density was approximately 15% higher in the test bioreactor than that in the control bioreactor (Fig. 3d). This difference can be attributed to run-to-run variation. Right before recirculation was started on day 4, cell density in the test bioreactor was already 11% higher than the control bioreactor.

LDH Release, Cell Size, and Apoptosis

Cell growth and viability results under repetitive exposure to 6.4×10^6 W/m^3 (Fig. 3d) was somewhat surprising. The

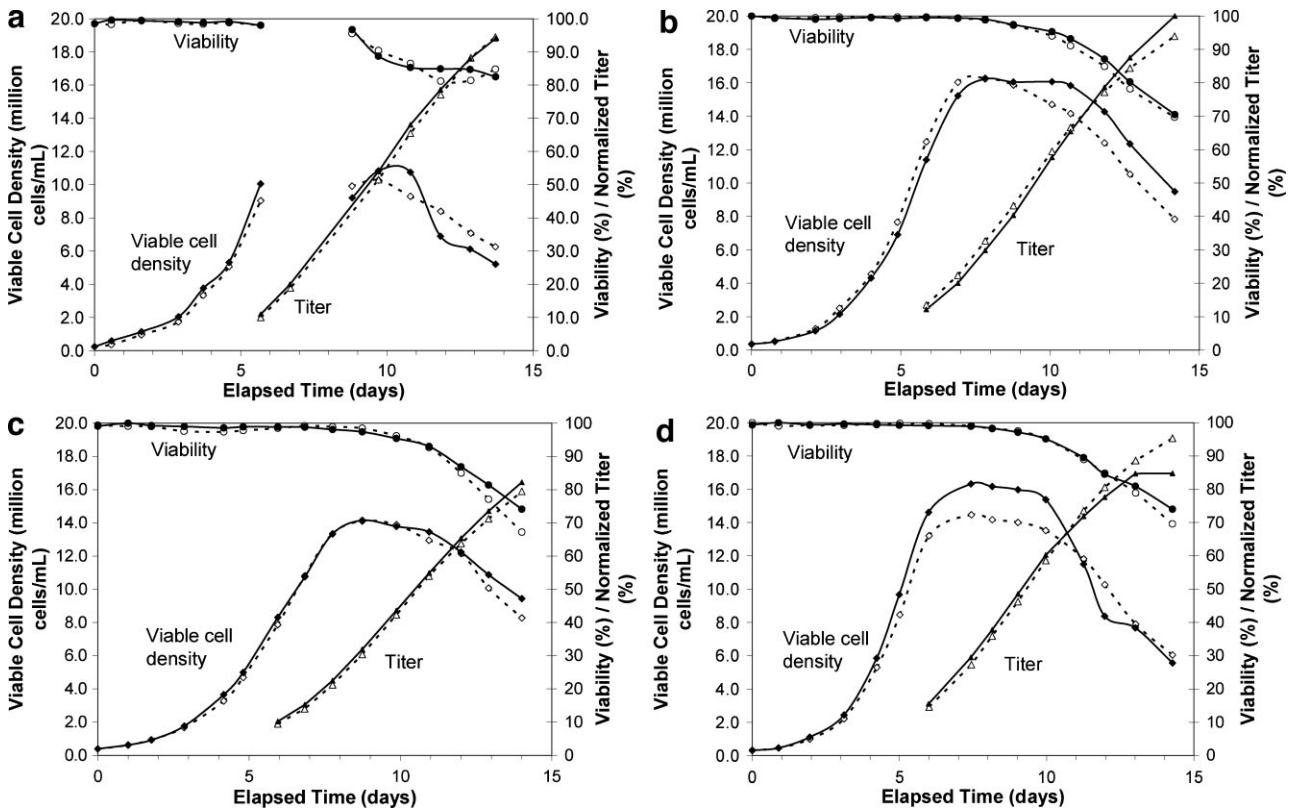

Figure 3. Viable cell density, viability, and normalized product titer in the test bioreactors where cells passed through the torture chamber in the recirculation loop (solid lines) and in the control bioreactors where cells were pumped through the recirculation loop without a torture chamber in it (dotted lines). Four sets of experiments, at four different EDR levels were studied: 6.0×10^4 (**a**), 2.9×10^5 (**b**), 2.3×10^6 (**c**), and 6.4×10^6 (**d**) W/m^3.

single exposure study showed that at 6.4×10^6 W/m^3, there was a roughly 0.5% increase in LDH release compared to the baseline, as shown in Figure 2b. If LDH release resulted purely from cell lysis, a 0.5% cell lysis per passage would represent a killing rate of 0.43 day^{-1} in the repetitive exposure bioreactor based on an average exposure frequency of 72 day^{-1}. This killing rate is significant compared to the net cell growth rate of 0.69 day^{-1} during the exponential growth phase. However, Figure 3d showed that after exposure was started on day 4, neither cell growth rate nor viability was affected in the test bioreactor. To reconcile single exposure and chronic exposure results, supernatant LDH concentration in the three highest EDR pairs of chronic exposure test and control bioreactors was measured and compared. Figure 4a and b demonstrates that at 2.9×10^5 W/m^3 and 2.3×10^6 W/m^3, supernatant LDH concentration was similar between the test and control bioreactors both before and after repetitive exposure started on day 4. However, at 6.4×10^6 W/m^3, there was an immediate increase in supernatant LDH after exposure started (Fig. 4c). This result is in good agreement with the single exposure experiment which showed elevated LDH at 6.4×10^6 W/m^3, but not at 2.9×10^5 W/m^3 and 2.3×10^6 W/m^3. In addition, at 6.4×10^6 W/m^3 the average cell diameter in the test bioreactor was smaller compared to the control bioreactor (Fig. 4c). In contrast, cell size in the two lower levels of energy dissipation rates was similar between the test and control bioreactors (Fig. 4a and b).

Results shown in Figures 3d and 4c can be summarized that under 6.4×10^6 W/m^3 repetitive exposure: (1) the net cell growth rate was not affected, (2) viability was not affected, (3) LDH released into the culture medium increased, and (4) cell size was reduced. These observations seem to suggest that at 6.4×10^6 W/m^3, the cell membrane might be disrupted which led to release of intracellular components into the medium; nevertheless, cells stayed viable and maintained the same net growth and production rate. Another plausible explanation is the selective disruption of large cells or cells in aggregates under 6.4×10^6 W/m^3, which could result in smaller average cell diameter and higher medium LDH level. Regardless which hypothesis is correct, the comparable net cell growth rate and product titer between cells under 6.4×10^6 W/m^3 exposure and cells in the control bioreactor demonstrated the strong resistance of CHO cells to intensive hydrodynamic abuse.

Early apoptotic and late apoptotic/necrotic cell populations during the fed-batch process were also monitored. The

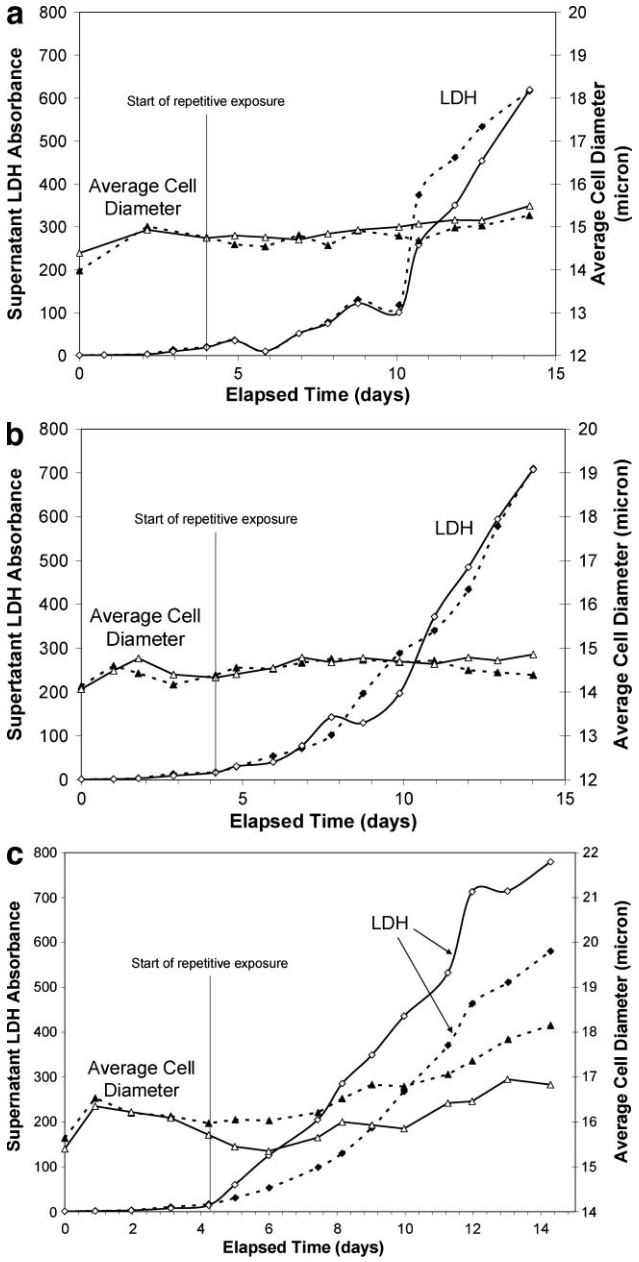

Figure 4. Comparison of supernatant LDH concentration and average cell diameter between the corresponding control (dotted lines) and test (solid lines) bioreactors during the fed-batch process. **a**: 2.9×10^5 W/m^3, (**b**) 2.3×10^6 W/m^3, (**c**) 6.4×10^6 W/m^3.

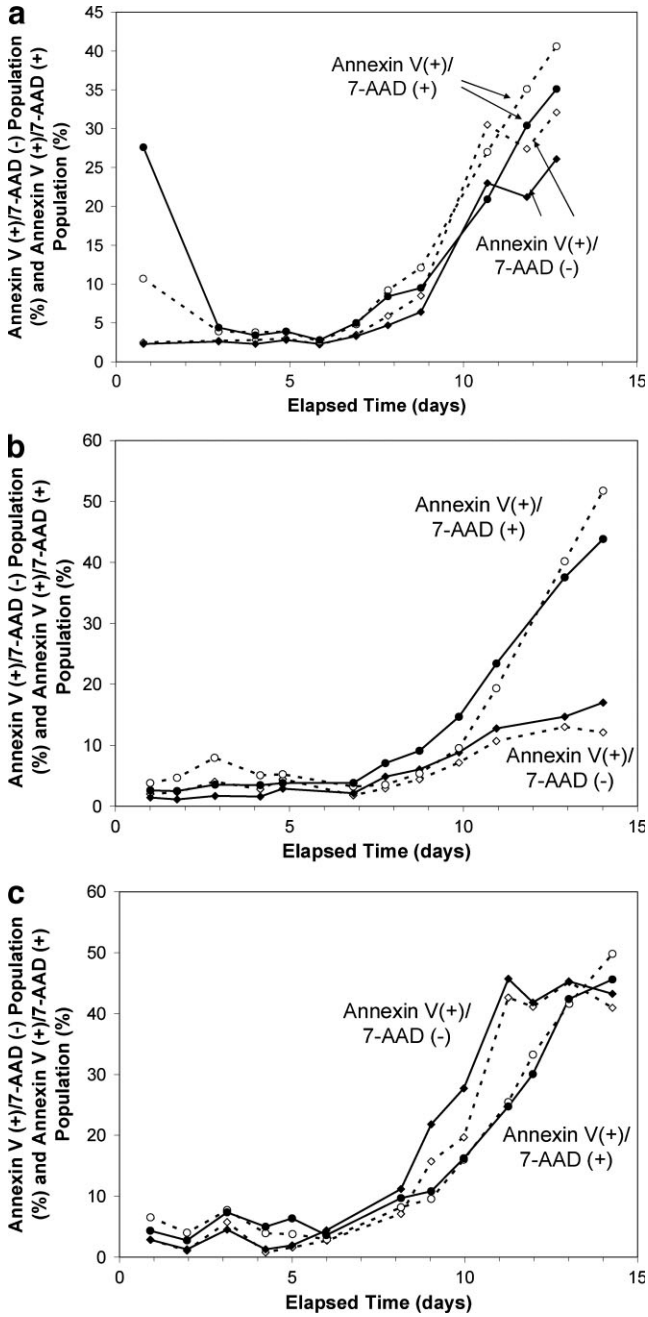

Figure 5. Comparison of early apoptotic population, Annexin V (+)/7-AAD (−), and late apoptotic/necrotic population, Annexin V (+)/7-AAD (+), between corresponding test (solid lines) and control (dotted lines) bioreactors. **a**: 2.9×10^5 W/m^3, (**b**) 2.3×10^6 W/m^3, (**c**) 6.4×10^6 W/m^3.

comparison of the three highest EDR pairs of test and control bioreactors is presented in Figure 5. Generally no significant difference between each pair of bioreactors was observed. It was also generally observed that the timing that early apoptotic and late apoptotic/necrotic cell populations started to increase coincided with the timing at which viable cell density started to drop based on trypan blue quantitation. Figure 5b (2.3×10^6 W/m^3) showed significantly lower early apoptotic population in both test and control bioreactors compared to Figure 5a (2.9×10^5 W/m^3) and Figure 5c (6.4×10^6 W/m^3). This correlates to the slower net cell growth rate and the later timing to reach peak cell density as compared to the other two pairs (Fig. 3); however, the exact reason for the lower early apoptotic population at slower net growth rate is unknown. Although immediate LDH release was observed after 6.4×10^6 W/m^3

exposure started (Fig. 4c) in the test bioreactor, neither early apoptotic nor late apoptotic/necrotic population in the test bioreactor was different from the control bioreactor (Fig. 5c).

Glucose Metabolism

The cumulative glucose consumption and lactic acid production, normalized to their respective maximum, in all four sets of tests are shown in Figure 6. The profiles of both glucose consumption and lactate production are very similar between each pair of test and control bioreactors at all four EDR levels. In all bioreactor runs, lactate concentration increased during the exponential growth phase. One day before reaching stationary phase, net lactate production switched to net consumption until all lactate was consumed. Based on the glucose and lactate results, we can infer that the amount of glucose entering the Krebs cycle through pyruvate was similar between the test and control bioreactors. Results shown in Figure 6 indicated that energy dissipation as high as 6.4×10^6 W/m^3 did not significantly affect glucose metabolism.

Product Quality

Four assays were used to assess the effects of repetitive hydrodynamic force on product heterogeneity. These assays were SDS–PAGE (reduced and non-reduced) for protein size and fragmentation, iCE for protein charge, peptide map for methionine oxidation, and organic SEC Mass Spectrometry for N-linked glycosylation.

Neither reduced nor non-reduced SDS–PAGE results revealed any difference between test and control bioreactor products at all four levels of energy dissipation rates. Gel images comparing products from the 6.4×10^6 W/m^3 exposure test are shown in Figure 7. The band pattern and band intensity between the test and control bioreactor samples were comparable in both non-reduced and reduced gel images.

Results of the other three assays are summarized in Table II. iCE is an imaged capillary isoelectric focusing assay for the quantification of charge profiles where acidic and basic species refer to products with either lower or higher isoelectric focusing point than the main product. Under all test conditions, no significant change of charge profile between control and test bioreactors was observed.

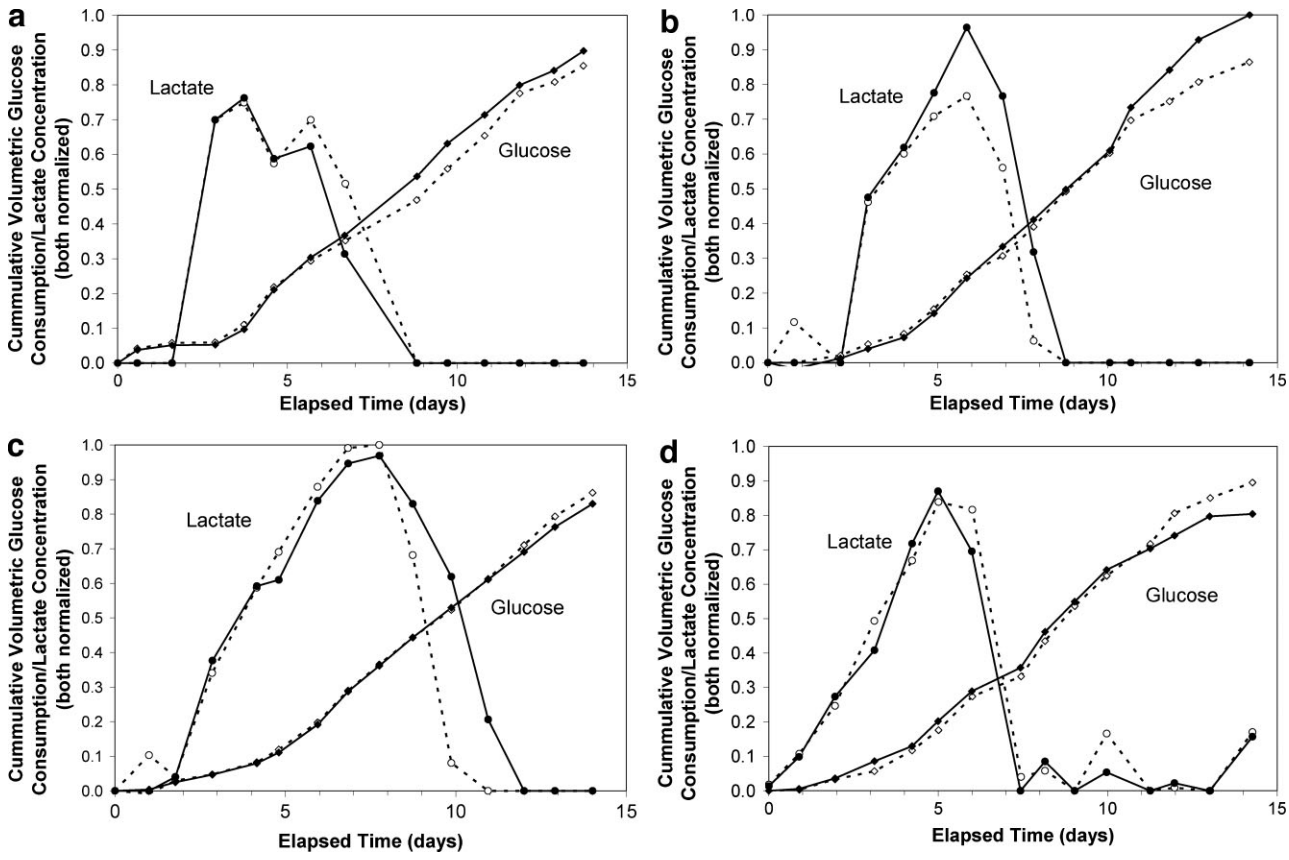

Figure 6. Comparison of glucose metabolism in corresponding control (dotted lines) and test (solid lines) bioreactors. **a**: 6.0×10^4 W/m^3, (**b**) 2.9×10^5 W/m^3, (**c**) 2.3×10^6 W/m^3, (**d**) 6.4×10^6 W/m^3. Glucose metabolism was based on cumulative volumetric glucose consumption and lactate concentration. All data are normalized to the highest lactate concentration and glucose consumption among all bioreactors.

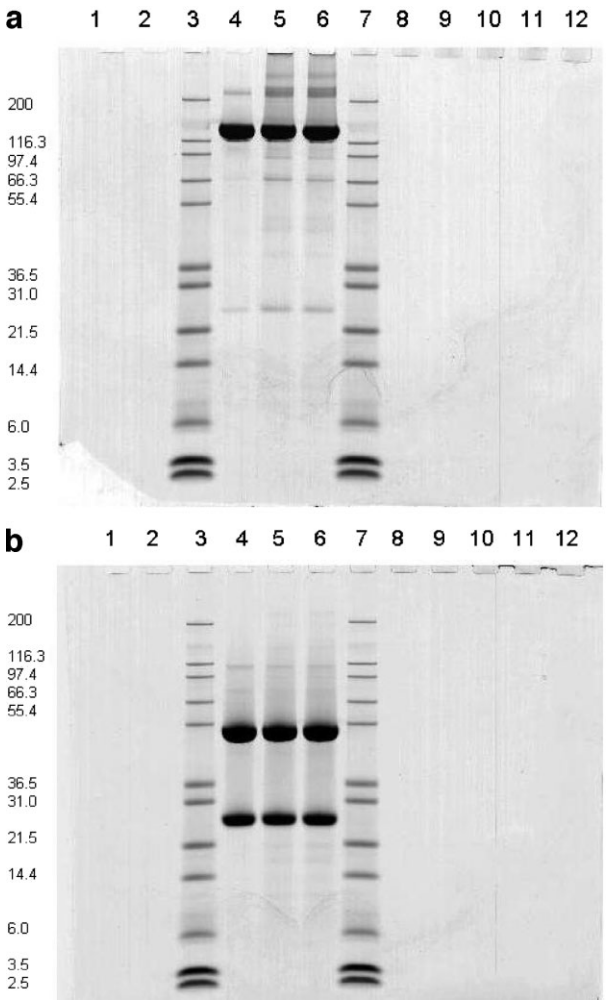

Lane	Material
3	Molecular weight marker
4	Standard
5	Control bioreactor material
6	Test bioreactor material
7	Molecular weight marker

Lane	Material
3	Molecular weight marker
4	Standard
5	Control bioreactor material
6	Test bioreactor material
7	Molecular weight marker

Figure 7. Comparison of product molecular weight and fragmentation of mAbs produced in the test and control bioreactors at 6.4×10^6 W/m^3. (**a**): Non-reduced and (**b**) reduced SDS–PAGE images.

Table II. Charge heterogeneity, methionine oxidation, and glycosylation results of recombinant antibodies produced in all control and test bioreactors. The ratios of each product quality attribute between the corresponding pair of test and control bioreactors are also included.

		Assay						
		Charge heterogeneity			Metionine oxidation	Glycosylation		
Energy dissipation rate (W/m^3)	Sample	Acidic isoforms	Main isoforms	Basic isoforms	Met-Ox	G0	G1	G2
6.0×10^4	Test bioreactor (%)	28.5	56.8	14.7	6.9	49.5	32.2	5.7
	Control bioreactor (%)	29.2	54.7	16.1	6.5	81.6	8.5	1.4
	Ratio of test/control	0.98	1.04	0.91	1.06	0.61	3.79	3.98
2.9×10^5	Test bioreactor (%)	27.0	60.0	13.0	3.7	60.6	30.1	5.3
	Control bioreactor (%)	25.4	57.5	17.2	3.3	82.1	9.5	0.9
	Ratio of test/control	1.07	1.04	0.76	1.12	0.74	3.16	6.12
2.3×10^6	Test bioreactor (%)	27.3	60.0	12.7	3.8	61.0	30.4	4.2
	Control bioreactor (%)	27.0	61.5	11.6	3.5	74.5	17.6	1.7
	Ratio of test/control	1.01	0.98	1.10	1.09	0.82	1.72	2.41
6.4×10^6	Test bioreactor (%)	33.8	56.5	9.7	5.4	55.1	31.8	5.6
	Control bioreactor (%)	26.1	59.3	14.6	6.0	80.0	9.3	1.0
	Ratio of test/control	1.30	0.95	0.66	0.90	0.69	3.43	5.50
1.2×10^1	Test bioreactor (%)	29.9	57.9	12.2	4.1	73.0	9.2	0.3
9.0×10^1	Test bioreactor (%)	26.9	58.5	14.6	4.8	73.6	9.0	1.5

The percentage of a specific methionine being oxidized in the mAb was monitored by a peptide map assay on reverse phase HPLC. The results, listed in Table II, showed variations among different sets of experiments. At 6.0×10^4 W/m^3 and 6.4×10^6 W/m^3, the oxidation level of mAbs from both the test and control bioreactors is around 6% while it was at about 3.5% for the two sets of middle level EDR samples. The variation was likely due to the storage duration difference of unpurified samples. Nevertheless, within each set of experiments, the results between the test and control bioreactors are very similar. This indicates that methionine oxidation was not affected by energy dissipation rate up to 6.4×10^6 W/m^3.

Three glycoforms, G0, G1, and G2, accounted for the majority of all glycoforms quantified by the organic SEC Mass Spectrometry. Of these three, G0 is the most dominant one while G2 is the least populous. As can be seen in Table II and Figure 8, while cells were under hydrodynamic stress, the distribution of these three glycoforms was significantly skewed toward G1 and G2. The four control bioreactors, although with different flow rates from 3 to 50 mL/min, performed similarly; therefore, only the average and 1× standard deviation was shown in Figure 8. The average of three historical runs without external recirculation loop was also included in Figure 8. The historical results were similar to those of the control bioreactors. Compared to both controls, G0 percentage in the test conditions was generally reduced from ~80% to ~55% while that of G1 and G2 was increased significantly from ~10% to ~30% and from ~1% to ~5% respectively. A similar shift of glycosylation pattern under hydrodynamic stress was observed using a second CHO clone producing a different test monoclonal antibody. Under 2.9×10^5 W/m^3 stress, G0 population of the second clone decreased from 73.8% to 59.9% while G1 and G2 populations increased from 19.8% and 1.7% to 27.8% and 4.2% respectively compared to corresponding control bioreactor populations.

Further Control Studies

An argument has been made that this shift in glycosylation pattern could be an artifact of the TC, since all control bioreactors did not include the TC in the circulation loop. A second set of control studies were added where two low EDR TCs were incorporated in the circulation loop of two control bioreactors. These two low EDR TCs had much wider flow channels: 1.5 and 2.0 mm in width. A flow rate in the middle range used with the 225 μm TC, 30 mL/min, generates a median, maximum EDR of 12 and 90 W/m^3 in the 1.5 and 2.0 mm TC respectively. Since all other components of the system were the same, when a recycle flow rate of 30 mL/min was used for each of the three TCs, the only difference was the median, maximum EDR (note, given the use of the same flow rates, the average exposures frequency is the same). Product quality results using the 1.5 and 2.0 mm TC (EDR of 12 and 90 W/m^3) are included in Table II and Figure 8. As illustrated clearly in Figure 8, glycosylation pattern was not affected using the low EDR TCs as compared to the patterns of the first set of controls and historical control results.

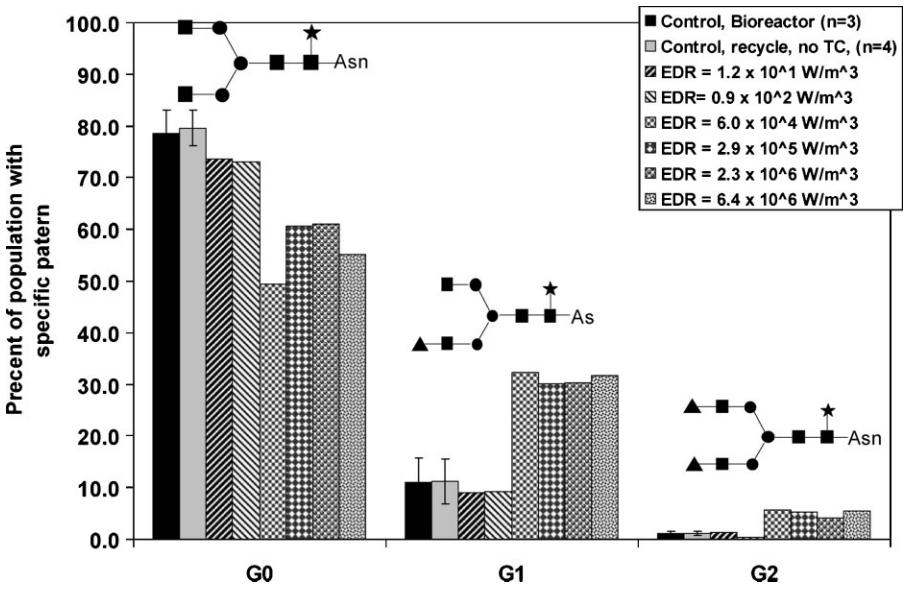

Figure 8. Glycosylation profiles of mAbs produced in all test and control bioreactors. Two sets of control results are included. One is the average of the four recirculating control bioreactors and the other one is the average of three historical non-recirculating bioreactors. The error bar indicates one standard deviation. (▲) galactose, (■) N-acetylglucosamine, (●) mannose, and (★) fucose.

Discussion

The bioreactor-recirculation system used in this study attempts to mimic the physical and nutritional environment that suspended cells experience in large-scale stirred tank bioreactors, which can be summarized in the following points. First, the fed-batch process in the bench-top bioreactor is the same as that executed in large-scale bioreactors with respect to nutritional environment, pH, dissolved oxygen, and temperature setpoints. Secondly, a repetitive high-low fluid dynamic stress environment that cells were subjected to in large-scale bioreactor is reproduced using the bench-scale bioreactor, TC system. The energy dissipation rate in the bench-scale bioreactor is low, a volumetric average rate of 10 W/m^3, and the local, maximum rate around the impellers is approximately 1.0×10^3 W/m^3. Conversely, the median, maximum energy dissipation rate generated in the torture chamber in this study can range from 1.2×10^1 to 6.4×10^6 W/m^3.

The two major differences/questions between this bioreactor-recirculation, TC system and large-scale bioreactors is exposure frequency and whether the high EDR created in the torture chamber is really similar to high levels of EDR created in a bioreactor. The flow rates tested in this study were 3, 10, 30, and 50 mL/min, which correspond to average exposure intervals of 200, 100, 33, and 20 min. These intervals are theoretically much longer than that in large-scale bioreactors (in min). However, it is suggested that the possibility that the frequency difference would change the results is low for a number of reasons. First, recirculation was continuous for an extended period of time (10 days), so that even with a low exposure frequency, the overall number of exposures was high. Second, glycosylation results showed no "dose response": 3 mL/min yielded the same level of glycosylation shift as 50 mL/min; yet its exposure frequency was much lower.

In the single exposure test, where LDH release was used to assess cell damage, the threshold energy dissipation rate for lethal cell damage was determined to be 2.3×10^6 W/m^3. This observation is similar to the sensitivity of most other mammalian cell lines in suspension (Ma et al., 2002) that have been tested with the TC.

In the repetitive exposure test, LDH release difference between the test and control bioreactors was not observed until EDR was higher than 2.3×10^6 W/m^3. Therefore, the threshold EDR for LDH release in the single and repetitive exposure test was the same, which demonstrates the relevance of single exposure model using LDH release to detect cell damage.

Interestingly, LDH release at multiple exposure to EDR of 6.4×10^6 W/m^3 (Fig. 4c) was not correlated to a decrease of cell viability, cell number, or product titer, but to a decrease of average cell diameter. Plausible explanations are cell "shrinkage" under hydrodynamic stress and the selective killing of large cells or cells in aggregates. The reduction of average cell size in a highly agitated CHO culture has been previously presented in public meetings by an industrial organization; however, we are not aware of any published studies on this observation. It is surprising that the test CHO cells can maintain the same level of physiological function and product formation capacity after a significant reduction in size. This is contrast to the results of Godoy-Silva et al. (2009) in which immediate release in LDH, and drop in both viable cells and total cells was initiated in this same recirculation system when an EDR of 2.3×10^6 W/m^3 was used. It should be noted that this previous study by Godoy et al. used the CHO line CHO6E6 purchased from ATTC (No. CRL-11398). In contrast, this study used an industrially relevant, and commonly used, CHO cell lines. Clearly, and not surprisingly, the cell line used in this study is more robust.

In contrast to the decrease in cell size at the highest level of repetitive EDR exposure, we did not detect any significant changes in glucose consumption and lactate production. This is in contrast to the results of Keane et al. (2003) who observed that at 0.8 N/m^2 (6.4×10^2 W/m^3), glucose uptake increased by 42% and to the results of McDowell and Papoutsakis (1998) who found that by increasing the agitation of a 2 L bioreactor from 80 rpm to 300–400 rpm, glucose consumption of HL60 cells increased by 40%. While it is important to note that the studies of Keane et al. were on a CHO line attached to a surface, the study of McDowell and Papoutsakis used suspended cells.

The effects on product quality are mixed. While no significant impacts on methionine oxidation, charge profile, and protein molecular weight and fragmentation were observed up to 6.4×10^6 W/m^3, glycosylation changed at a much lower EDR, 6.0×10^4 W/m^3. It is not surprising to find the glycosylation change, but it is surprising to find that the change is actually toward the more completely glycosylated direction and the change was dose independent over two orders of EDR magnitude between 6.0×10^4 W/m^3 and 6.4×10^6 W/m^3. Compared to the materials generated in the control bioreactors, G0 population decreased while those of G1 and G2 increased. This shift suggests that hydrodynamic stress actually improves CHO cell's glycosylation capability. The glycosylation shift was not observed at a median, maximum EDR of 0.9×10^2 W/m^3 or lower using the wider TC channels. Finally, a similar shift in glycosylation pattern was observed using a second CHO clone producing a different test antibody when the cells were under repetitive 2.9×10^5 W/m^3 stress.

The link between cause and effect is unknown, but one possible mechanism involves integrin activation. Integrins are cell surface receptors for cells to attach to extra cellular matrix. It is also a major mechanical force sensor for cells, whose activation could trigger multiple signal transductions, including one that leads to actin cytoskeleton polymerization (DeMali et al., 2003). It has been reported that actin dynamics can change Golgi apparatus's structural organization (Egea et al., 2006). When mammalian cells were treated with an actin toxin to depolymerize actin cytoskeleton, swelling of Golgi cisternae was observed, indicating the functional role of actin

cytoskeleton in maintaining the flat morphology of Golgi cisternae (DeMali et al., 2003). Because the spatial distribution of glycosylation enzymes in Golgi relies heavily on morphology, actin polymerization may improve Golgi apparatus's structure and hence glycosylation capability.

To our knowledge, there is no prior report on the effect of hydrodynamic force on glycosylation pattern shift. While Senger and Karim (2003) claimed that occupancy level of N-linked glycosylation site on tPA produced by CHO cells decreased with increased agitation, they did not report any changes in glycoslyation structure. In this study, N-glycosylation occupancy level was not monitored.

Ma et al. (2002) and Mollet et al. (2007) previously compared the hydrodynamic sensitivity of several mammalian cell lines, characterized by cell lysis or LDH release, to the hydrodynamic forces generated in stirred tanks. These comparisons have shown that although bubble rupture could cause immediate cell lysis, the energy dissipation from typical agitation is significantly (many orders of magnitude) below the level that can cause cell death. This study adds a new dimension to this comparison. Figure 9 is a summary figure, modified from Mollet et al. (2007), in which the previously reported EDR that can cause death of animal cells, as well as EDR values for a variety of bioprocess

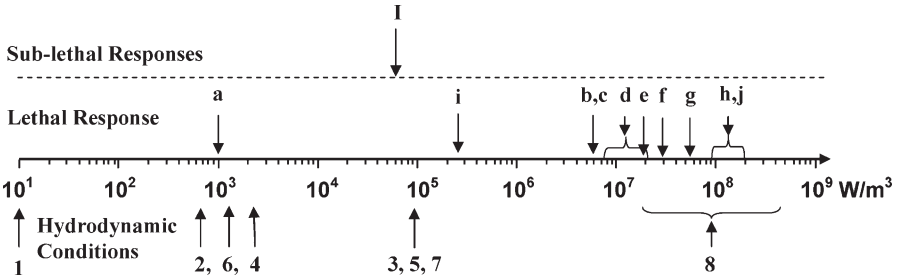

Sub-lethal Physiological Responses Critical to Bioprocesses

Symbol	Cell	Mode of growth	Mode of test	Response	Reference
I	CHO	Suspended	10 days repetitive exposure	Recombinant protein Glycosylation profile change	This study

Lethal Responses (necrosis including LDH release)

Symbol	Cell	Mode of growth	Reference
a	CHO-K1	Anchoraged for growth and test	Gregoriades (2000)
b	PER.C6	Suspended (naïve or adenovirus infected)	Ma (2002)
c	CHO (GS)	Suspended	This study
d	Hybridoma	Suspended	Thomas et al. (1994); Zhang et al. (1993)
e	MCF-7	Suspended	Ma et al. (2002)
f	Mouse myeloma	Suspended	McQueen and Bailey (1989)
g	Hela S3, mouse L929	Suspended	Augenstein et al. (1971)
h	CHO-K1, Hybridoma HB-24	Suspended	Ma et al. (2002)
i	CHO-K1, apoptosis	Anchoraged for growth, suspended during test	Mollet et al. (2007)
j	CHO-K1	Suspended (wild type and bcl2 transfected)	Mollet et al. (2007)

Hydrodynamic Conditions

Symbol	Process	Description	Reference
1	Agitation	Volume average energy dissipation rate in typical animal cell culture bioreactors	Varley and Birch (1999)
2	Agitation	Volume average energy dissipation rate in a 10L mixing vessel (Rushton Turbine impeller, 700 RPM)	Zhou and Kresta (1996a)
3	Agitation	Maximum local energy dissipation rate in a 10L mixing vessel (Rushton Turbine impeller, 700 RPM)	Zhou and Kresta (1996a)
4	Agitation	Volume average energy dissipation rate in a 22,000L fermentor (Rushton Turbine impeller, 140 RPM)	Wernersson and Tragardh (1999)
5	Agitation	Maximum local energy dissipation rate in a 22,000L fermentor (Rushton Turbine impeller, 140 RPM)	Wernersson and Tragardh (1999)
6	Agitation	Maximum local energy dissipation rate in a spinner vessel	Venkat et al. (1996)
7	Bubble rupture	Pure water (bubble diameter: 6.32 mm)	Garcia-Briones et al. (1994)
8	Bubble rupture	Pure water (bubble diameter: 1.7 mm)	Boulton-Stone and Blake (1993) Garcia-Briones et al. (1994)

Figure 9. Comparison of cell responses to the hydrodynamic forces generated in agitated and sparged bioreactors. The comparison includes results from this as well as previously published studies.

conditions are presented. To Figure 9 we have added the minimum value of EDR that we observed the glycosylation pattern shift in this study. As can be visually observed, this EDR value is two orders of magnitude lower than that to cause cell lysis as measured by LDH release.

The maximum EDR in a typically, well mixed vessel is approximately 100 times the bulk, mean EDR value (Mollet et al., 2004). For typical large-scale bioreactors with volumetric average power input on the order of 10 W/m^3 (Varley and Birch, 1999), the maximum EDR from agitation would be on the order of 10^3 W/m^3, which is one order magnitude lower than the level at which glycosylation shift was triggered. In addition, we used median, maximum EDR values to characterize the hydrodynamic stress in the torture chamber. This is a conservative approach as most impacts should be observed well before half of the cells were exposed to a specific EDR. Therefore, although this study indicated that physiological responses can be triggered by EDR much lower than that required to physically kill the cells, one can not conclude that this physiological response will occur in typical large-scale stirred tank bioreactors without follow-up studies and model confirmations.

As a next step, we want to test the clone in a 30 L bioreactor in which EDR values at or above the level that this study indicates a change in glycosylation pattern will occur. Mollet et al. (2004) predicts that an RPM of on the order of 400–500 would be needed to achieve the lowest level of EDR reported in this study that caused the glycosylation pattern shift. In the mean time, we want to test the cells in the range of 1×10^3–6.0×10^4 W/m^3, which is more representative of the hydrodynamic stress in large-scale stirred tank bioreactors.

The authors appreciate Ellen McCormick, Dave Brunner, Amit Banerjee, and Michele Bailey Piatchek for their critical review of the manuscript, members of Process Development Analytics group for conducting all analytical assays, Michael Dupuis for purifying the products, and Culture Process Development group for various assistances during the study.

References

Al-Rubeai M, Singh RP, Goldman MH, Emery AN. 1995. Death mechanisms of animal cells in conditions of intensive agitation. Biotechnol Bioeng 45:463–472.

Augenstein DC, Sinskey AJ, Wang DIC. 1971. Effect of shear on the death of two strains of mammalian tissue cells. Biotechnol Bioeng 13:409–418.

Boulton-Stone JM, Blake JR. 1993. Gas bubbles bursting at a free surface. J Fluid Mech 254:437–466.

Chalmers JJ. 2000. Animal cell culture, effects of agitation and aeration on cell adaptation. In: Spier R, Griffiths JB, Scragg AH, editors. Encyclopedia of cell technology. New York: Wiley. pp. 41–51.

Chisti Y. 1999. Shear sensitivity. In: Flickinger MC, Drew SW, editors. Encyclopedia of bioprocess technology: Fermentation, biocatalysis, and bioseparation, vol. 5. New York: Wiley. pp. 2379–2406.

Chisti Y. 2000. Animal-cell damage in sparged bioreactors. Trends Biotechnol 18:420–432.

Datamonitor Plc, Monoclonal antibodies report part I. Reference code DMHC2291. 2007.

DeMali KA, Wennerberg K, Burridge K. 2003. Integrin signaling to the actin cytoskeleton. Curr Opin Cell Biol 15:572–582.

Egea G, Lazaro-Dieguez F, Vilella M. 2006. Actin dynamics at the Golgi complex in mammalian cells. Curr Opin Cell Biol 18:168–178.

Garcia-Briones MA, Brodkey RS, Chalmers JJ. 1994. Computer simulations of the rupture of a gas bubble at a gas-liquid interface and its implications in animal cell damage. Chem Eng Sci 49:2301–2320.

Godoy-Silva R, Mollet M, Chalmers JJ. 2009. Evaluation of the effect of chronic hydrodynamical stresses on cultures on suspension of CHO cells. Biotechnol Bioeng 102:1119–1130.

Gregoriades N, Clay J, Ma N, Koelling K, Chalmers JJ. 2000. Cell damage of microcarrier cultures as a function of local energy dissipation created by a rapid extensional flow. Biotechnol Bioeng 69:171–182.

Hu W, Gladue R, Hansen J, Wojnar C, Chalmers JJ. 2007. The sensitivity of the Dinoflagellate Crypthecodinium cohnii to transient hydrodynamic forces. Biotechnol Prog 23:1355–1362.

Joshi JB, Elias CB, Patole MS. 1996. Role of hydrodynamic shear in the cultivation of animal, plant and microbial cells. Chem Eng J 62:121–141.

Keane JT, Ryan D, Gray PP. 2003. Effect of shear stress on expression of a recombinant protein by Chinese hamster ovary cells. Biotechnol Bioeng 81:211–220.

Ludwig A, Tomeczkowski J, Kretzmer G. 1992. Influence of shear stress on adherent mammalian cells during division. Biotechnol Lett 14:881–884.

Ma N. 2002. Quantitative studies of the bubble-cell interactions and the mechanisms of mammalian cell damage from hydrodynamic forces. Ph.D. Dissertation. The Ohio State University.

Ma N, Koelling KW, Chalmers JJ. 2002. Fabrication and use of a transient, contractional flow device to quantify the sensitivity of mammalian and insect, cells to hydrodynamic forces. Biotechnol Bioeng 80:428–437.

Ma N, Mollet M, Chalmers JJ. 2006. Aeration, mixing and hydrodynamics in bioreactors. In: Ozturk S, Hu W, editors. Cell culture technology for pharmaceutical and cell-based therapies. NY: Marcel Dekker. pp. 2379–2406.

McDowell CL, Papoutsakis ET. 1998. Increased agitation intensity increases CD13 receptor surface content and mRNA levels, and alters the metabolism of HL60 cells cultured in stirred tank bioreactors. Biotechnol Bioeng 60:239–250.

McQueen A, Bailey JE. 1989. Influence of serum level, cell-line, flow type and viscosity on flow-induced lysis of suspended mammalian-cells. Biotechnol Lett 11:531–536.

McQueen A, Meilhoc E, Bailey JE. 1987. Flow effects on the viability and lysis of suspended mammalian cells. Biotechnol Lett 9:831–836.

Mollet M, Ma N, Zhao Y, Brodkey R, Taticek R, Chalmers JJ. 2004. Bioprocess equipment: Characterization of energy dissipation rate and its potential to damage cells. Biotechnol Prog 20:1437–1448.

Mollet M, Godoy-Silva R, Berdugo C, Chalmers JJ. 2007. Acute hydrodynamic forces and apoptosis: A complex question. Biotechnol Bioeng 98:772–788.

Motobu M, Wang P, Matsumura M. 1998. Effect of shear stress on recombinant Chinese hamster ovary cells. J Ferment Bioeng 85:190–195.

Ranjan V, Waterbury R, Xiao Z, Diamond SL. 1996. Fluid shear stress induction of the transcriptional activator c-fos in human and bovine cells, HeLa and Chinese hamster ovary cells. Biotechnol Bioeng 49:383–390.

Senger RS, Karim MN. 2003. Effect of shear force on intrinsic CHO culture state and glycosylation of recombinant tissue-type plasminogen activator protein. Biotechnol Prog 19:1199–1209.

Thomas CR, Al-Rubeai M, Zhang Z. 1994. Prediction of mechanical damage to animal cells in turbulence. Cytotechnology 15:329–335.

Varley J, Birch J. 1999. Reactor design for large-scale suspension animal cell culture. Cytotechnology 29:177–205.

Venkat RV, Stock LR, Chalmers JJ. 1996. Study of hydrodynamics in microcarrier culture spinner vessels: A particle tracking velocimetry approach. Biotechnol Bioeng 49:456–466.
Vickroy B, Lorenz K, Kelly W. 2007. Modeling shear damage to suspended CHO cells during cross-flow filtration. Biotechnol Prog 23:194–199.
Wernersson ES, Tragardh C. 1999. Scale-up of Rushton turbine-agitated tanks. Chem Eng Sci 54:4245–4256.
Wurm F. 2004. Production of recombinant protein therapeutics in cultivated mammalian cells. Nature Biotechnol 22:1393–1398.
Zhang Z, Al-Rubeai M, Thomas CR. 1993. Estimation of disruption of animal cells by turbulent capillary flow. Biotechnol Bioeng 42:987–993.
Zhou G, Kresta SM. 1996a. Impact of tank geometry on the maximum turbulence energy dissipation rate for impellers. AIChE J 42:2476–2490.
Zhou G, Kresta SM. 1996b. Distribution of energy between convective and turbulent flow for three frequently used impellers. Chem Eng Res Deg 74:379–389.